

Article

Magnesium and Calcium Transport along the Male Rat Kidney: Effect of Diuretics

Pritha Dutta ^{1,*}  and Anita T. Layton ^{1,2,3,4}

¹ Department of Applied Mathematics, University of Waterloo, Waterloo, ON N2L 3G1, Canada; anita.layton@uwaterloo.ca

² Cheriton School of Computer Science, University of Waterloo, Waterloo, ON N2L 3G1, Canada

³ Department of Biology, University of Waterloo, Waterloo, ON N2L 3G1, Canada

⁴ School of Pharmacy, University of Waterloo, Waterloo, ON N2L 3G1, Canada

* Correspondence: p7dutta@uwaterloo.ca

Abstract: Calcium (Ca^{2+}) and magnesium (Mg^{2+}) are essential for cellular function. The kidneys play an important role in maintaining the homeostasis of these cations. Their reabsorption along the nephron is dependent on distinct trans- and paracellular pathways and is coupled to the transport of other electrolytes. Notably, sodium (Na^+) transport establishes an electrochemical gradient to drive Ca^{2+} and Mg^{2+} reabsorption. Consequently, alterations in renal Na^+ handling, under pathophysiological conditions or pharmacological manipulations, can have major effects on Ca^{2+} and Mg^{2+} transport. One such condition is the administration of diuretics, which are used to treat a large range of clinical conditions, but most commonly for the management of blood pressure and fluid balance. While the pharmacological targets of diuretics typically directly mediate Na^+ transport, they also indirectly affect renal Ca^{2+} and Mg^{2+} handling through alterations in the electrochemical gradient. To investigate renal Ca^{2+} and Mg^{2+} handling and how those processes are affected by diuretic treatment, we have developed computational models of electrolyte transport along the nephrons. Model simulations indicate that along the proximal tubule and thick ascending limb, the transport of Ca^{2+} and Mg^{2+} occurs in parallel with Na^+ , but those processes are dissociated along the distal convoluted tubule. We also simulated the effects of acute administration of loop, thiazide, and K-sparing diuretics. The model predicted significantly increased Ca^{2+} and Mg^{2+} excretions and significantly decreased Ca^{2+} and Mg^{2+} excretions on treatment with loop and K-sparing diuretics, respectively. Treatment with thiazide diuretics significantly decreased Ca^{2+} excretion, but there was no significant alteration in Mg^{2+} excretion. The present models can be used to conduct in silico studies on how the kidney adapts to alterations in Ca^{2+} and Mg^{2+} homeostasis during various physiological and pathophysiological conditions, such as pregnancy, diabetes, and chronic kidney disease.

Keywords: calcium homeostasis; magnesium homeostasis; electrolyte transport; kidney; renal transport



Citation: Dutta, P.; Layton, A.T. Magnesium and Calcium Transport along the Male Rat Kidney: Effect of Diuretics. *Math. Comput. Appl.* **2024**, *29*, 13. <https://doi.org/10.3390/mca29010013>

Academic Editors: Weizhong Dai and Sundeep Singh

Received: 16 October 2023

Revised: 22 January 2024

Accepted: 4 February 2024

Published: 7 February 2024



Copyright: © 2024 by the authors. Licensee MDPI, Basel, Switzerland. This article is an open access article distributed under the terms and conditions of the Creative Commons Attribution (CC BY) license (<https://creativecommons.org/licenses/by/4.0/>).

1. Introduction

The divalent cations, Ca^{2+} and Mg^{2+} , are important for various physiological processes. About 99% of the body's Ca^{2+} is stored in bones, where it forms a calcium-phosphate compound called hydroxyapatite [1]. The remaining 1% of body calcium plays an important role in various other physiological processes, such as cell signaling, both skeletal and smooth muscle contraction, and blood clotting [1]. Mg^{2+} plays a pivotal role in energy-demanding metabolic reactions, protein synthesis, ensuring membrane integrity, facilitating nervous tissue conduction, promoting neuromuscular excitability, regulating muscle contraction, influencing hormone secretion, and participating in intermediary metabolism. Nearly 99% of the body's Mg^{2+} is distributed within cells or stored in bone, with only a small fraction in circulation [2]. Tight regulation of the serum Ca^{2+} and Mg^{2+} concentrations is essential since too much or too little Ca^{2+} or Mg^{2+} can have dangerous, potentially fatal consequences. To maintain Ca^{2+} and Mg^{2+} balance, it is crucial to regulate the fluxes of Ca^{2+}

and Mg^{2+} among the primary organs involved in their regulation, namely the intestine, bone, and kidneys.

The kidneys play an important role in maintaining Mg^{2+} and Ca^{2+} homeostasis. The majority, ~60–70% of the filtered Ca^{2+} , is reabsorbed along the proximal tubule through the paracellular pathway [3]. By contrast, paracellular Mg^{2+} permeability in the proximal tubule is very low, and hence only 15–25% of the filtered Mg^{2+} is reabsorbed along this segment [3]. The majority of the filtered Mg^{2+} is reabsorbed along the cortical thick ascending limb (60–70%) paracellularly [3]. The paracellular fractional reabsorption of Ca^{2+} along the thick ascending limb is ~15–25% [3]. The distal convoluted tubule is the final segment that reabsorbs Mg^{2+} ; hence, it plays an important role in fine-tuning urinary Mg^{2+} excretion. Approximately 5–10% of the filtered Mg^{2+} is reabsorbed transcellularly along the distal convoluted tubule, mediated by the transient receptor potential melastatin 6/7 (TRPM6/7) heteromeric complex on the apical membrane and the Na^+/Mg^{2+} exchanger on the basolateral membrane [3]. Approximately 5–10% of the filtered Ca^{2+} is reabsorbed transcellularly along the distal convoluted tubule and connecting tubule, mediated by the transient receptor potential vanilloid 5 (TRPV5) on the apical membrane, the Na^+/Ca^{2+} exchanger (NCX1), and plasma membrane Ca^{2+} -ATPase (PMCA) on the basolateral membrane [3]. Finally, ~2–5% of the filtered Mg^{2+} and Ca^{2+} are excreted through urine [3].

Our understanding of Ca^{2+} and Mg^{2+} handling within different segments of the nephron has been greatly advanced through micropuncture and microperfusion studies in rodent nephrons [4,5]. Furthermore, recent genetic studies have expanded our knowledge about the protein mediators of Ca^{2+} and Mg^{2+} transport [6]. Despite these advances, our understanding of the renal handling of these electrolytes remains incomplete. What fraction of the renal reabsorption goes through the transcellular versus paracellular pathway? To what extent is the renal transport in each nephron segment coupled to the transport of other electrolytes, e.g., Na^+ , K^+ , and Cl^- ? To answer these questions, we developed a detailed computational model of epithelial transport of electrolytes and water along the nephrons in a male rat kidney and conducted simulations to predict the renal transport of Ca^{2+} and Mg^{2+} as well as other electrolytes and water under different physiological conditions.

Besides electrolyte and fluid homeostasis, the kidney also plays an essential role in maintaining normal blood pressure. For the management of blood pressure and fluid balance, diuretics are commonly prescribed. Although the pharmacological targets of diuretics directly affect Na^+ transport, they also indirectly affect renal Mg^{2+} and Ca^{2+} reabsorption through changes in the electrochemical gradient. How is renal Ca^{2+} and Mg^{2+} transport affected by the administration of diuretics? To answer this question, we simulate the effect of acute administration of three classes of diuretics—loop; thiazide; and K-sparing diuretics—on renal Mg^{2+} and Ca^{2+} transport and excretion.

2. Materials and Methods

We have previously developed epithelial cell-based computational models of transporter-mediated solute and water transport along the nephron of a rat kidney [7–10], focusing on the renal handling of Na^+ , K^+ , Ca^{2+} , glucose, and water in physiological and pathophysiological conditions. The superficial nephron model includes the proximal tubule, short descending limb, thick ascending limb, distal convoluted tubule, connecting tubule, and collecting duct segments. Each nephron segment is represented as a tubule lined by a layer of epithelial cells. The model tracks the transport of the following 17 solutes: Na^+ , K^+ , Cl^- , HCO_3^- , H_2CO_3 , CO_2 , NH_3 , NH_4^+ , HPO_4^{2-} , $H_2PO_4^-$, H^+ , HCO_2^- , H_2CO_2 , urea, glucose, Ca^{2+} , and Mg^{2+} . The segment and cell type determine the type and abundance of transporters found on the apical and basolateral membranes of the cell. Solutes and water may be transported across the epithelium by either moving across the apical and basolateral membranes in the transcellular pathway, mediated by specialized membrane transporters or channels, or via the paracellular pathway between neighboring cells. A schematic diagram for the model nephrons is shown in Figure 1.

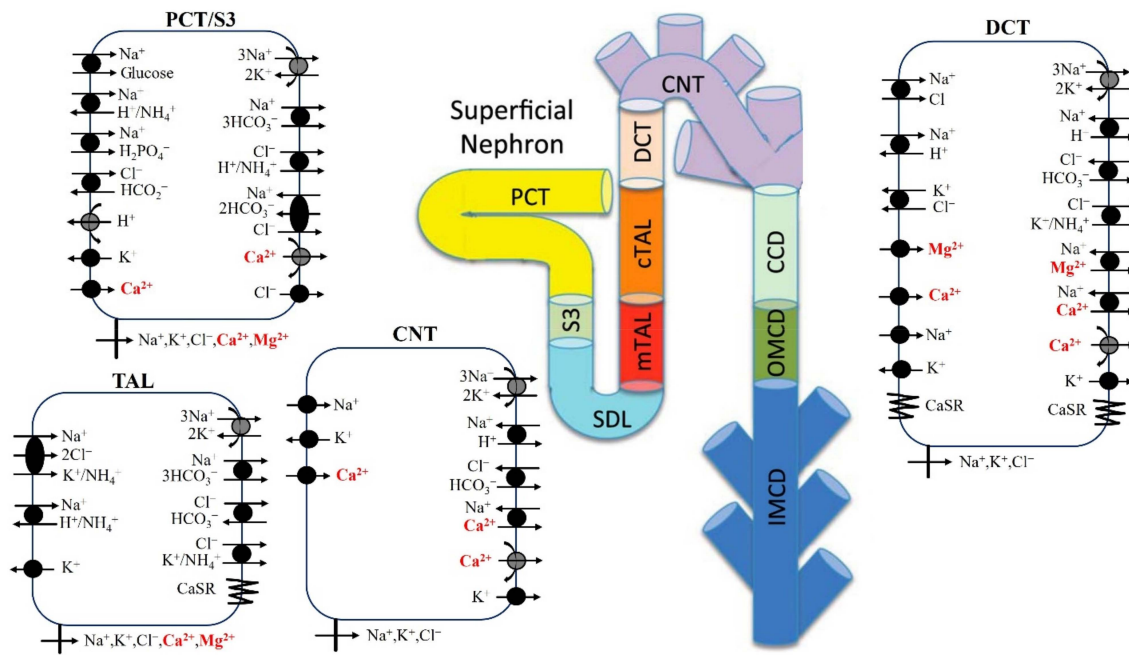


Figure 1. Model diagram of epithelial transport of Ca^{2+} and Mg^{2+} and selected electrolytes along the superficial nephron. Mg^{2+} transport occurs along the proximal tubule (proximal convoluted tubule, PCT, and S3), cortical thick ascending limb (cTAL), and distal convoluted tubule (DCT). Ca^{2+} transport occurs along the proximal tubule (proximal convoluted tubule, PCT, and S3), medullary/cortical thick ascending limb (mTAL/cTAL), distal convoluted tubule (DCT), and connecting tubule (CNT). Only the major Na^+ , K^+ , Cl^- , Ca^{2+} , and Mg^{2+} transporters are shown. PCT, proximal convoluted tubule; SDL, short descending limb; mTAL, medullary thick ascending limb; limb; CNT, connecting tubule; CCD, cortical collecting duct; OMCD, outer-medullary collecting duct; IMCD, inner-medullary collecting duct.

The model is defined by a large system of coupled differential and algebraic equations that describe mass conservation and determine transmembrane and paracellular fluxes [11]. The model predicts luminal fluid flow, hydrostatic pressure, membrane potential, luminal and cytosolic solute concentrations, transcellular and paracellular fluxes, urine volume, and urinary excretion rates of model solutes.

Below, we summarize a model representation of Mg^{2+} transport along the proximal tubule, cortical thick ascending limb, and distal convoluted tubule. Model parameters that describe Mg^{2+} transport are given in Table 1. The analogous model description and parameter for Ca^{2+} transport can be found in Ref. [10]. Additional model parameters can be found in Ref. [12].

2.1. Mg^{2+} Transport along the Proximal Tubule

The proximal tubule reabsorbs 15–25% of the filtered Mg^{2+} load through the paracellular pathway, which is mediated by claudin-2 and -12 [13] and is driven by the favorable electrochemical gradient established by Na^+/H^+ exchanger 3 (NHE3)-mediated Na^+ reabsorption [5,14,15]. Paracellular electro-diffusive Mg^{2+} flux ($J_{\text{Mg}}^{\text{PT,LI}}$) is given by

$$J_{\text{Mg}}^{\text{PT,LI}} = P_{\text{Mg}}^{\text{PT,LI}} \zeta_{\text{Mg}}^{\text{LI}} \left(\frac{C_{\text{Mg}}^{\text{L}} - C_{\text{Mg}}^{\text{I}} e^{-\zeta_{\text{Mg}}^{\text{LI}}}}{1 - e^{-\zeta_{\text{Mg}}^{\text{LI}}}} \right), \quad (1)$$

where the superscripts L and I denote lumen and lateral intercellular space (LIS), respectively; $P_{\text{Mg}}^{\text{PT,LI}}$ denotes the permeability of Mg^{2+} at the lumen and LIS interface; $\zeta_{\text{Mg}}^{\text{LI}} = \frac{Z_{\text{Mg}} F}{RT} (\psi^{\text{L}} - \psi^{\text{I}})$; Z_{Mg} is the valence of Mg^{2+} (+2); C_{Mg}^{L} and C_{Mg}^{I} denote Mg^{2+} concentrations in the lumen and LIS, respectively; ψ^{L} and ψ^{I} denote the luminal and LIS membrane potentials, respectively; $RT = 2.57 \text{ J/mmol}$; and $F = 96.5 \text{ C/mmol}$ represents Faraday's constant.

2.2. Mg^{2+} Transport along the Thick Ascending Limb

The medullary thick ascending limb has negligible Mg^{2+} reabsorption [15–17]. In contrast, the cortical thick ascending limb reabsorbs 60–70% of the filtered Mg^{2+} via the paracellular route. That flux is mediated by claudins 16 and 19 [18], and is driven by the electrochemical gradient established by $Na^+K^+Cl^-$ cotransporter 2 (NKCC2)-mediated Na^+ transport [9,14]. Paracellular Mg^{2+} transport in the cortical thick ascending limb $J_{Mg}^{cTAL,LI}$ is represented by an expression analogous to Equation (1), with the superscript “PT” replaced by “cTAL”.

2.3. Mg^{2+} Transport along the Distal Convoluted Tubule

Unlike the proximal tubule and cortical thick ascending limb, where Mg^{2+} transport proceeds passively via the paracellular route, the reabsorptive process along the distal convoluted tubule is active and transcellular and is mediated by the TRPM6 and TRPM7 (TRPM6/7) heteromeric channels, expressed on the apical membranes [19]. Mg^{2+} flux through TRPM6/7 is given by

$$J_{Mg}^{TRPM6/7} = N_{TRPM6/7} \times f_{Mg} \times f_{pH} \times \frac{\Delta\psi^{LC} - E_{Mg}^{LC}}{2F}, \quad (2)$$

f_{Mg} and f_{pH} describe the effects of intracellular Mg^{2+} concentration (C_{Mg}^C) and extracellular pH on TRPM6/7 [20], and are given by

$$f_{Mg} = \frac{1}{1 + \left(\frac{C_{Mg}^C}{0.51}\right)^2}. \quad (3)$$

$$f_{pH} = g_{pH7.4} \left(2 - \frac{1}{1 + \frac{7.4 - pH^L}{7.4 - pH_{1/2}^L}} \right), \quad (4)$$

where $g_{pH7.4}$ denotes the single channel conductance of TRPM6/7 channel at pH 7.4, pH^L denotes the luminal fluid pH, and $pH_{1/2}$ denotes the luminal fluid pH for half-maximal conductance.

Mg^{2+} efflux through the basolateral membrane is assumed to be mediated by an Na^+/Mg^{2+} exchanger [19,21], given by

$$J_{Mg}^{NaMgX} = J_{Mg}^{NaMgX,max} \times f_{NaS} \times f_{NaC} \times f_{MgS} \times f_{MgC}, \quad (5)$$

where $J_{Mg}^{NaMgX,max}$ denotes the maximum Mg^{2+} flux through the Na^+/Mg^{2+} exchanger,

and the f terms represent regulation by extracellular Na^+ , $f_{NaS} = \frac{(c_{Na}^S)^2}{((c_{Na}^S)^2 + (K_{M,NaS})^2)}$,

intracellular Na^+ , $f_{NaC} = \frac{K_{M,NaC}}{(c_{Na}^C + K_{M,NaC})}$, extracellular Mg^{2+} , $f_{MgS} = \frac{K_{M,MgS}}{(c_{Mg}^S + K_{M,MgS})}$, and

intracellular Mg^{2+} , $f_{MgC} = \frac{(c_{Mg}^C)^2}{((c_{Mg}^C)^2 + (K_{M,MgC})^2)}$. In these expressions, $K_{M,NaS}$, $K_{M,NaC}$,

$K_{M,MgS}$, and $K_{M,MgC}$ denote the Michaelis-Menten constants.

2.4. Calcium-Sensing Receptor

The calcium-sensing receptor (CaSR) regulates not only Ca^{2+} and Mg^{2+} reabsorption in the kidneys but other electrolytes and water as well by modifying transporter activities. Ca^{2+} is the primary ligand for activating CaSR. At equimolar concentrations, Mg^{2+} is 1/2 to 2/3 as potent as Ca^{2+} in activating CaSR [22,23]. We model the effect of CaSR on a given parameter v (v may denote paracellular permeability, NKCC2 activity, ROMK activity, or NCC activity; see below) with the following expression:

$$v = v^* \left(1 + \alpha_{v,Ca} \left(\frac{(C_{Ca}^i)^4}{(C_{Ca}^i)^4 + (EC_{50,Ca})^4} \right) \right) \left(1 + \alpha_{v,Mg} \left(\frac{(C_{Mg}^i)^4}{(C_{Mg}^i)^4 + (EC_{50,Mg})^4} \right) \right), \quad (6)$$

where v^* is the value of v in the absence of the effect of CaSR, c_{Ca}^i and c_{Mg}^i denote the concentration of Ca^{2+} and Mg^{2+} in the luminal ($i = L$) or interstitial ($i = S$) fluid, and $EC_{50,Ca} = 1.25$ mM and $EC_{50,Mg} = 2.5$ mM represent the half-maximal concentrations for Ca^{2+} and Mg^{2+} [24], respectively. CaSR is ubiquitously expressed in the kidney both along the apical and basolateral membranes, with its highest expression being at the basolateral membrane of the cortical thick ascending limb [25]. Hence, we represent v for (i) paracellular permeability, NKCC2 activity, and renal outer-medullary potassium channel (ROMK) in the thick ascending limb, (ii) $Na^+ - Cl^-$ cotransporter (NCC) activity in the distal convoluted tubule, (iii) $H^+ - ATPase$ flux in outer-medullary collecting duct type A cells, and (iv) water permeability in the inner-medullary collecting duct. The parameters $\alpha_{v,Ca}$ and $\alpha_{v,Mg}$ are negative if CaSR has an inhibitory effect on v and positive otherwise. Since the effect of Mg^{2+} on CaSR activation is $\sim 50\text{--}66\%$ of that of Ca^{2+} , we set $\alpha_{v,Mg} = 0.6\alpha_{v,Ca}$. The values for $\alpha_{v,Ca}$ and $\alpha_{v,Mg}$ for each of the segments are given in Table 1.

Table 1. Mg^{2+} -specific parameters for all the segments along the superficial nephron. Values marked (*) are adjusted. PT, proximal tubule; TAL, thick ascending limb; DCT, distal convoluted tubule; CD, collecting duct; OMCD, outer-medullary collecting duct; IMCD, inner-medullary collecting duct.

Parameter	Value
PT	
Tight junction permeability to Mg^{2+} at the lumen-LIS interface ($P_{Mg}^{PT,LIS}$)	1.1×10^{-5} cm/s [26]
Reflection coefficient of tight junction to Mg^{2+}	0.89 (*)
cTAL	
Tight junction permeability at the lumen-LIS interface in the absence of Mg^{2+} ($P_{Mg}^{TAL,LIS}$)	38×10^{-5} cm/s (*)
Maximum half concentration of Ca^{2+} ($EC_{50,Ca}$)	1.25 mM [24]
Maximum half concentration of Mg^{2+} ($EC_{50,Mg}$)	2.5 mM [24]
Hill function coefficient, n	4 [24]
Inhibitory coefficient of Ca^{2+} on tight junction permeability ($\alpha_{P,Ca}$)	$-4/7$ [27]
Inhibitory coefficient of Mg^{2+} on tight junction permeability ($\alpha_{P,Mg}$)	-0.34 (*)
Inhibitory coefficient of Ca^{2+} on NKCC2 activity ($\alpha_{NKCC2,Ca}$)	-0.4 [28]
Inhibitory coefficient of Mg^{2+} on NKCC2 activity ($\alpha_{NKCC2,Mg}$)	-0.24 (*)
Inhibitory coefficient of Ca^{2+} on ROMK activity ($\alpha_{ROMK,Ca}$)	-0.8 [29,30]
Inhibitory coefficient of Mg^{2+} on ROMK activity ($\alpha_{ROMK,Mg}$)	-0.48 (*)
DCT	
TRPM6/7 channel density ($N_{TRPM6/7}$)	26×10^4 cm ⁻² (*)
Single channel conductance of TRPM6/7 at pH 7.4 ($g_{pH7.4}$)	56.6 pS [20]
Luminal pH for half-maximal conductance of TRPM6/7 ($pH_{1/2}$)	5.5 [20]
Maximum Mg^{2+} flux through Na^+ / Mg^{2+} exchanger ($J_{Mg}^{NaMgX,max}$)	8.6×10^{-9} mmol/cm ² /s (*)
Intracellular Mg^{2+} half-saturation constant ($K_{M,MgC}$)	3.59 M [19,21]
Extracellular Mg^{2+} half-saturation constant ($K_{M,MgS}$)	1.3 mM [19,21]
Intracellular Na^+ half-saturation constant ($K_{M,NaC}$)	12.29 mM [19,21]
Extracellular Na^+ half-saturation constant ($K_{M,NaS}$)	87.5 mM [19,21]
Excitatory coefficient of Ca^{2+} on NCC activity ($\alpha_{NCC,Ca}$)	0.5 [31]
Excitatory coefficient of Mg^{2+} on NCC activity ($\alpha_{NCC,Mg}$)	0.3 (*)
CD	
Ca^{2+} promoting coefficient for apical HATPase activity of type A OMCD cells ($\alpha_{HATP,Ca}$)	2 [27]
Mg^{2+} promoting coefficient for apical HATPase activity of type A OMCD cells ($\alpha_{HATP,Mg}$)	1.2 (*)
Ca^{2+} inhibitory coefficient for apical water permeability of IMCD cells ($\alpha_{Pf,Ca}$)	$-3/8$ [27]
Mg^{2+} inhibitory coefficient for apical water permeability of IMCD cells ($\alpha_{Pf,Mg}$)	-0.225 (*)

3. Results

3.1. Baseline Results

Using rat parameters, we computed the model's luminal fluid flow, luminal fluid solute concentrations, cytosolic solute concentrations, membrane potential, and fluxes. Figure 2 shows the predicted segmental delivery, transport, and luminal fluid concentration of Mg^{2+} and Ca^{2+} along the nephron. Results for other electrolytes and water can be found in Ref. [32].

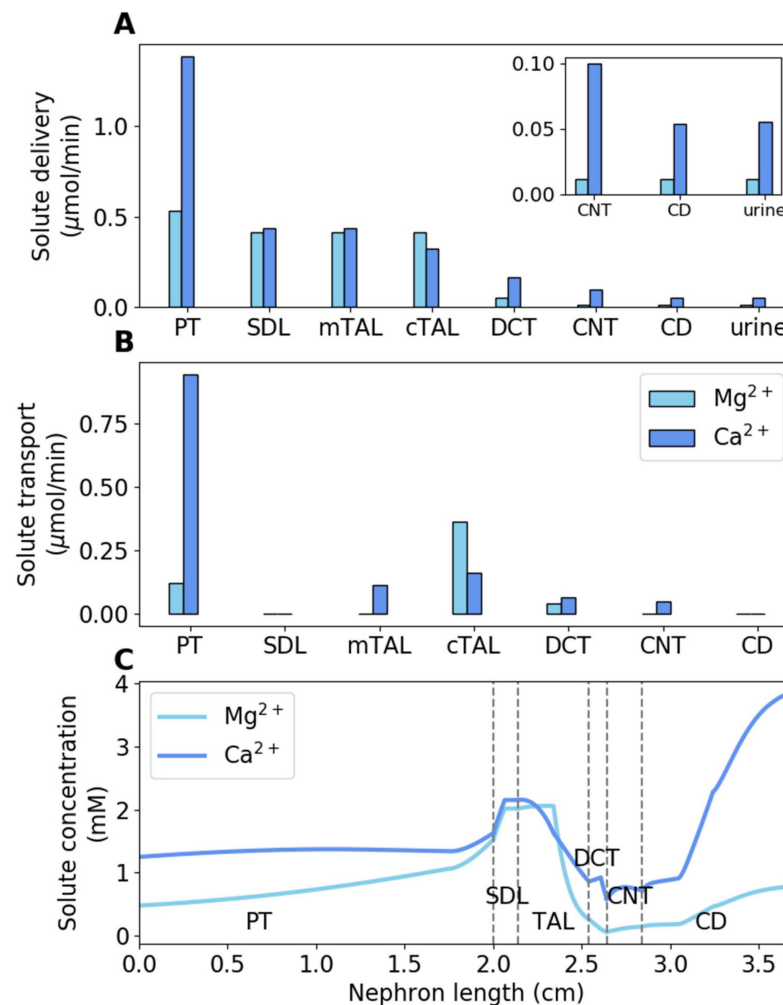


Figure 2. Baseline results. (A) Delivery of Mg^{2+} and Ca^{2+} to key nephron segments in male rats, given per kidney. (B) Mg^{2+} and Ca^{2+} transepithelial transport along key nephron segments in male rats, given per kidney. (C) Luminal Mg^{2+} and Ca^{2+} concentrations along key nephron segments in male rats. PT, proximal tubule; SDL, short descending limb; mTAL, medullary thick ascending limb; limb; cTAL, cortical thick ascending limb; DCT, distal convoluted tubule; CNT, connecting tubule; CD, collecting duct.

The majority of the filtered Ca^{2+} is reabsorbed along the proximal tubule, accounting for 68% of the filtered load; by contrast, Mg^{2+} reabsorption along this segment accounts for only 22% of the filtered load. Since Mg^{2+} reabsorption is low along the proximal tubule, Mg^{2+} concentration increases by ~ 3 -fold [4]. The majority of the overall Mg^{2+} transport occurs downstream along the cortical thick ascending limb (68% of the filtered load), where the lumen-positive membrane potential drives Mg^{2+} reabsorption via the paracellular pathway. The fractional reabsorption of Ca^{2+} along the medullary and cortical thick ascending limb is 20%. The final nephron segment that transports Mg^{2+} is the distal convoluted tubule, where 6.6% of the filtered Mg^{2+} is reabsorbed. The fractional reabsorption of Ca^{2+} along the distal convoluted tubule and connecting tubule is 7.9%. Finally, fractional urinary Mg^{2+} and Ca^{2+} excretions are 3.2% and 3.9%, respectively.

3.2. Effect of Loop Diuretics

Loop diuretics inhibit NKCC2, which is expressed on the apical membrane of the thick ascending limb. We simulated the effect of acute administration of loop diuretics by inhibiting NKCC2 activity by 70%. We assumed that the NKCC2 inhibitor was administered for long enough to significantly impair the kidney's ability to generate an axial osmolality gradient. The cortical interstitial concentrations were assumed to remain unchanged. Since the concentrating mechanism of the outer medulla is significantly impaired following complete NKCC2 inhibition, the interstitial concentrations of Mg^{2+} and Ca^{2+} at the outer-inner medullary boundary are lowered to 0.77 mM (from a baseline value of 0.96 mM) and 2.0 mM (from a baseline value of 2.5 mM), respectively. At the papillary tip, the interstitial concentrations of Mg^{2+} and Ca^{2+} are reduced to 1.0 mM (from 1.54 mM) and 2.62 mM (from 4.0 mM), respectively. For changes in the interstitial concentrations of Na^+ , K^+ , Cl^- , and urea, refer to [9].

The predicted Mg^{2+} and Ca^{2+} transport along the thick ascending limb and distal tubules and urinary Mg^{2+} and Ca^{2+} excretions following NKCC2 inhibition in male rats are shown in Figure 3. Our NKCC2 inhibition simulations predicted the fractional Mg^{2+} reabsorption along the cortical thick ascending limb to decrease to 57% from the baseline fractional reabsorption of 69% (Figure 3). Administration of furosemide, a loop diuretic, to male mice increased TRPM6 mRNA expression by 30% [33]. Our model simulations predicted a 68% increase in TRPM6/7 channel activity to account for the 240% increase in Mg^{2+} excretion in male rats undergoing furosemide treatment [34]. Fractional Ca^{2+} reabsorption along the thick ascending limb decreased by 17% following NKCC2 inhibition (Figure 3). This resulted in urinary Ca^{2+} excretion increasing to 236% of the baseline excretion value (Figure 3).

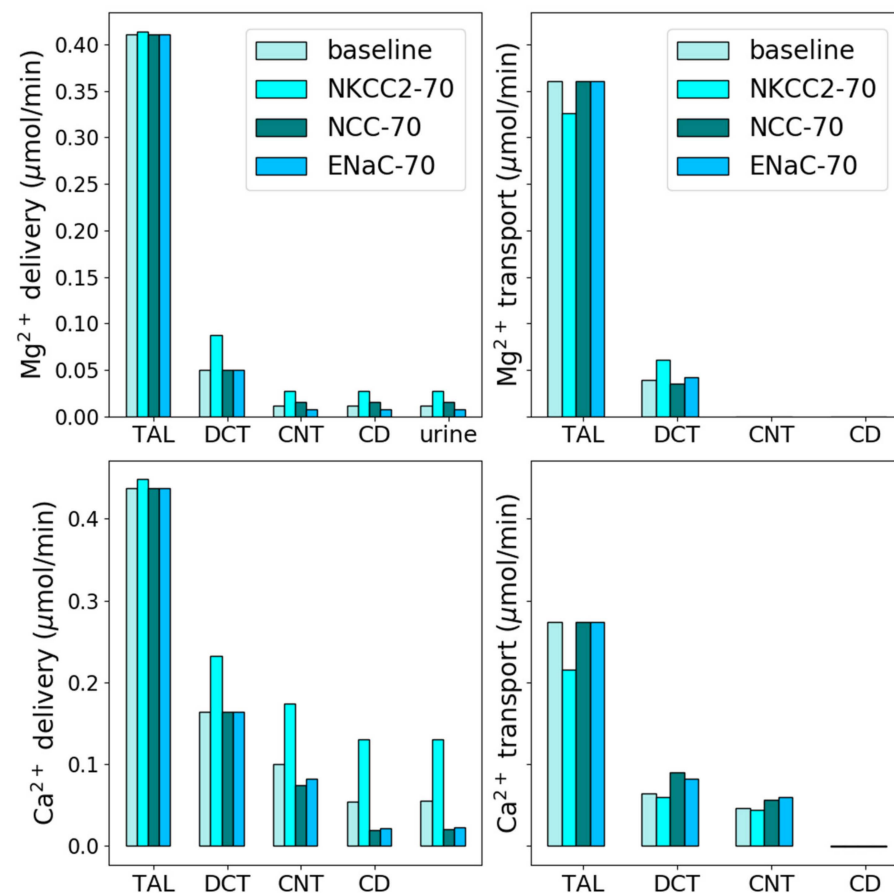


Figure 3. Effects of diuretic treatment. Delivery and transport of Mg^{2+} and Ca^{2+} along key nephron segments in male rats under normal conditions and 70% inhibition of NKCC2, NCC, and ENaC. The values are given per kidney. TAL, thick ascending limb; DCT, distal convoluted tubule; CNT, connecting tubule; CD, collecting duct.

3.3. Thiazide Diuretics

Thiazide diuretics inhibit NCC, which is expressed along the apical membrane of the distal convoluted tubule. We simulated the effect of acute administration of thiazide diuretics by inhibiting NCC activity by 70%. In the NCC inhibition simulations, baseline interstitial concentration profiles were used.

The predicted fractional Mg^{2+} excretion after NCC inhibition increased to 3.1% from the baseline value of 2.8% (Figure 3). This is in agreement with experimental data where male rats treated with bendrofluazide, a thiazide diuretic, did not show any significant change in Mg^{2+} excretion [35]. Acute administration of chlorothiazide to male mice increased TRPV5 mRNA expression by 40–80% and decreased Ca^{2+} excretion by ~60% [36]. Accordingly, we increased TRPV5 activity by 52% following NCC inhibition in our model. This decreased the predicted Ca^{2+} excretion by 63% from the baseline excretion value (Figure 3).

3.4. K-Sparing Diuretics

K-sparing diuretics, such as amiloride, block Na^+ uptake through ENaC, expressed on the apical membrane of the late distal convoluted tubule as well as along the full length of the connecting tubule and collecting ducts. In our model, we simulated the effect of K-sparing diuretics by reducing ENaC activity by 70%.

ENaC inhibition hyperpolarizes the luminal membrane potential and increases K^+ , Ca^{2+} , and Mg^{2+} uptake [37–40]. Our model simulations predicted Mg^{2+} reabsorption along the distal convoluted tubule to increase by 8.2% and Ca^{2+} reabsorption along the distal convoluted tubule and connecting tubule to increase by 29% (Figure 3). These increased reabsorptions decreased Mg^{2+} and Ca^{2+} excretions by 31% and 56%, respectively (Figure 3).

3.5. TRPM6/7 Inhibition

Kidney-specific TRPM6 [41] and TRPM7 [42] knock-out mice did not display hypomagnesemia and increased urinary Mg^{2+} excretion. This indicates that in mice, there must be other Mg^{2+} uptake mechanisms in the distal convoluted tubule. In fact, Verschuren et al. [43] reported that fluid shear stress (FSS) stimulated Mg^{2+} uptake in mDCT15 cells, and this uptake was independent of the TRPM6 and TRPM7 channels. However, the pathways or regulatory mechanisms for this FSS-sensitive Mg^{2+} uptake are unclear and hence not included in our present model.

To simulate TRPM6/7 knock-out experiments, we inhibited the TRPM6/7 channel by 100%. Our model predicted fractional Mg^{2+} excretion to increase to 8.8% (from baseline 3.2%), which is significantly above the 2–5% physiological fractional Mg^{2+} excretion. How much should the Mg^{2+} uptake through the FSS-sensitive Mg^{2+} channel be for fractional Mg^{2+} excretion to be within the physiological range when TRPM6/7 is completely inhibited? Our simulations predicted that if Mg^{2+} uptake through the FSS-sensitive channel is at least 60% of the Mg^{2+} uptake through TRPM6/7, then the fractional Mg^{2+} excretion becomes 4.3% (within the physiological range).

4. Discussion

Calcium (Ca^{2+}) and magnesium (Mg^{2+}) are both essential for cellular function. The homeostasis of these cations must be tightly regulated, and that balance is facilitated by intestinal absorption and renal excretion. For Na^+ , Cl^- , K^+ , Ca^{2+} , and many other major filtered solutes, most of the renal reabsorption occurs along the proximal convoluted tubule (about 1/2 to 2/3 in rats); the same is true for water. Thus, the luminal concentrations of these solutes, including Ca^{2+} , remain close to plasma along the proximal convoluted tubule. The majority of proximal tubule Ca^{2+} reabsorption occurs via a passive paracellular process, driven by Na^+ reabsorption mediated primarily by NHE3 and subsequent water reabsorption. In contrast, only 15–25% of the filtered Mg^{2+} load is reabsorbed along the proximal tubule. As a result, its concentration rises significantly along the proximal tubule. For Mg^{2+} , most of the reabsorption occurs along the cortical thick ascending limb (about 60–70%), while somewhat unexpectedly, essentially none occurs along the medullary

thick ascending limb. Most of the remainder of the Mg^{2+} is reabsorbed along the distal convoluted tubule.

What difference does it make for the cortical thick ascending limb and distal convoluted tubule to handle most of the Mg^{2+} transport instead of the proximal tubule, as in the case of Na^+ and Cl^- ? Having these distal segments responsible for transporting a substantial fraction of the filtered Mg^{2+} load via the pathways that can be regulated may give the kidney a better ability to regulate Mg^{2+} balance. Recall that the plasma Mg^{2+} level is orders of magnitude lower than Na^+ or Cl^- . Thus, to maintain plasma $[Mg^{2+}]$ within a narrow range, the ability to fine-tune renal Mg^{2+} transport is particularly crucial. Parathyroid hormone, for instance, increases Mg^{2+} reabsorption in both the cortical thick ascending limb and distal convoluted tubule [44]. Transport of Mg^{2+} along these segments can also be regulated by hormones such as calcitonin, vasopressin, glucagon, and β -adrenergic agonists [45]. Coincidentally, some common diuretics also target these segments.

The goal of this study is to better understand the impact of diuretics on renal Ca^{2+} and Mg^{2+} transport. Diuretics are medications that reduce fluid buildup in the body and are often employed in the management of hypertension, edema, and various other conditions influenced by changes in electrolyte transport. In the context of kidney function, diuretics often focus on transport proteins or mechanisms vital for the reabsorption of Na^+ , Cl^- , and water. Considering that renal Ca^{2+} and Mg^{2+} transports are driven primarily by the electrochemical gradients established by tubular NaCl transport processes, potential modifications in the renal handling of Ca^{2+} and Mg^{2+} by the administration of diuretics deserve scrutiny.

Loop diuretics, such as furosemide, induce notable natriuresis by targeting the thick ascending limb of the nephron; specifically, they inhibit NKCC2-dependent transport by competing for the chloride (Cl^-) binding site [46]. Given that the inhibition of NKCC2 reduces the lumen-positive transepithelial voltage gradient across the thick ascending limb epithelium [47], it is unsurprising that the transport of Mg^{2+} and Ca^{2+} in this segment is substantially decreased [48,49]. In fact, loop diuretics like furosemide induce hypercalciuria and hypermagnesuria in both experimental animals [50] and human subjects [51]. Thiazide diuretics induce a natriuretic response by inhibiting NCC and blocking NaCl transport in the distal convoluted tubule. A hypocalciuric effect has been reported following thiazide treatment [52]. Consistent with the drug's mode of action, among hypertensive individuals undergoing chronic thiazide treatment, there is a slight decrease in serum Mg^{2+} levels compared to those not taking diuretics [53], although the effect appears to be subtle. K-sparing diuretics function by inhibiting ENaC, a protein expressed in the late distal convoluted tubule, connecting tubule, and collecting duct of the kidney. Research has confirmed that K-sparing diuretics impact the urinary excretion of Ca^{2+} and Mg^{2+} in both human subjects and animals. Hypertensive individuals undergoing K-sparing diuretics treatment exhibit reduced urinary Ca^{2+} excretion [53] and elevated serum Mg^{2+} levels compared to those not receiving treatment [53]. The effect of these three classes of diuretics on urinary Mg^{2+} and Ca^{2+} excretions has been summarized in Figure 4.

The present study considers renal Ca^{2+} and Mg^{2+} transport under normal physiological conditions. The homeostasis of these electrolytes is altered during pregnancy, lactation, and dietary restriction, as well as in diseases such as diabetes and chronic kidney disease. To utilize the present model for *in silico* studies of how the kidney adapts in terms of Ca^{2+} and Mg^{2+} transport under these physiological and pathophysiological conditions, one can combine the model with computational models of kidney function for a pregnant rat [54,55], a diabetic rat [56–58], and a nephrectomized rat [8,59]. The resulting models may provide insights into altered renal Ca^{2+} and Mg^{2+} transport under these conditions. How do changes in renal Ca^{2+} and Mg^{2+} transport impact whole-body Ca^{2+} and Mg^{2+} homeostasis? A whole-body Ca^{2+} and Mg^{2+} balance model may help answer that question. By incorporating the present model into whole-body electrolyte balance models (e.g., [60–63]), one can obtain an integrative model to study whole-body Ca^{2+} and Mg^{2+} balance.

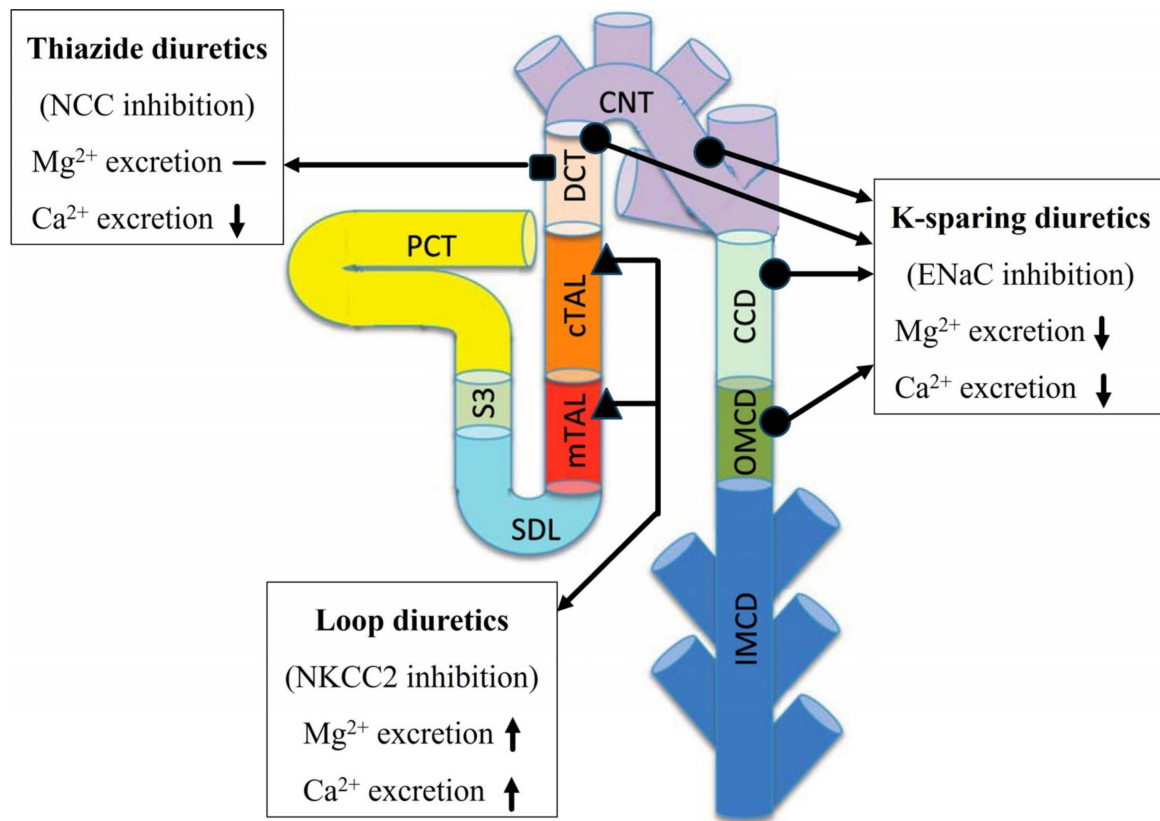


Figure 4. Summary of the effects of diuretic treatment. The effect of loop diuretics, thiazide diuretics, and K-sparing diuretics on Mg^{2+} and Ca^{2+} excretion. The upward arrow indicates an increase, the downward arrow indicates a decrease, and the dash indicates no significant change. Notations are analogous to Figure 1.

The present model simulates electrolyte and water transport along a superficial nephron, which constitutes only 2/3 of the total nephron population in a rat kidney. The juxtamedullary nephrons, whose loops of Henle extend into various depths of the inner medulla, comprise the remaining nephron population. These two types of nephrons differ in the single-nephron glomerular filtration rate, transport area, and transporter activities. This study focuses on a superficial nephron model to gain a clearer understanding of segmental Mg^{2+} transport. In future studies, developing a kidney model that incorporates both types of nephrons will enable more accurate predictions of urinary excretion rates.

Another limitation of this model is that it does not include cyclin and CBS domain divalent metal cation transport mediator 2 (CNNM2), expressed on the basolateral membrane, which is also potentially involved in Mg^{2+} transport along the distal convoluted tubule. CNNM2 has been shown to mediate both cellular Mg^{2+} influx and efflux. The role of CNNM2 as an Mg^{2+} transporter has been openly debated (in favor [64]; opposing view [65]). A common view is that CNNM2 is not a Mg^{2+} transporter by itself but is an important protein for regulating Mg^{2+} homeostasis [65,66]. Due to these conflicting views on the role of CNNM2 as a Mg^{2+} transporter, we did not include it in our present model. CNNM2 can be incorporated into our model in the future when more consistent experimental outcomes are available.

Author Contributions: Conceptualization, A.T.L.; Methodology, P.D. and A.T.L.; Software, Validation, Formal Analysis, and Investigation, P.D.; Resources, A.T.L.; Data Curation, P.D.; Writing—Original Draft, P.D. and A.T.L.; Writing—Review and Editing, P.D. and A.T.L.; Visualization, P.D.; Supervision, P.D. and A.T.L.; Funding Acquisition, A.T.L. All authors have read and agreed to the published version of the manuscript.

Funding: This research was funded by the Canada 150 Research Chair program, the National Sciences and Engineering Research Council of Canada (NSERC) Discovery Grant (Grant number: RGPIN-2019-03916), and the Canada Institutes of Health Research (CIHR) Project Grant (Grant number: TNC-174963) (to A.T.L.).

Data Availability Statement: The code used for this study can be accessed at https://github.com/Pritha17/Nephron-Mg_Ca_transport (16 October 2023).

Conflicts of Interest: The authors declare no conflicts of interest.

References

1. Pu, F.; Chen, N.; Xue, S. Calcium intake, calcium homeostasis and health. *Food Sci. Hum. Wellness* **2016**, *5*, 8–16. [CrossRef]
2. Taal, M.W.; Chertow, G.M.; Marsden, P.A.; Skorecki, K.; Alan, S.; Brenner, B.M. *Brenner and Rector's the Kidney E-Book*; Elsevier Health Sciences: Amsterdam, The Netherlands, 2011; ISBN 1-4557-2304-5.
3. Alexander, R.T.; Dimke, H. Effect of diuretics on renal tubular transport of calcium and magnesium. *Am. J. Physiol. Ren. Physiol.* **2017**, *312*, F998–F1015. [CrossRef]
4. Brunette, M.; Vigneault, N.; Carriere, S. Micropuncture study of magnesium transport along the nephron in the young rat. *Am. J. Physiol. Leg. Content* **1974**, *227*, 891–896. [CrossRef] [PubMed]
5. Le Grimellec, C.; Giocondi, M.C.; Philippe, P. Micropuncture study along the proximal convoluted tubule electrolyte reabsorption in first convolutions. *Pflug. Arch.* **1975**, *354*, 133–150. [CrossRef] [PubMed]
6. Curry, J.N.; Yu, A.S.L. Magnesium Handling in the Kidney. *Adv. Chronic Kidney Dis.* **2018**, *25*, 236–243. [CrossRef] [PubMed]
7. Layton, A.T.; Layton, H.E. A Computational Model of Epithelial Solute and Water Transport along a Human Nephron. *PLoS Comput. Biol.* **2018**, *15*, e1006108. [CrossRef] [PubMed]
8. Layton, A.T.; Vallon, V. SGLT2 Inhibition in a Kidney with Reduced Nephron Number: Modeling and Analysis of Solute Transport and Metabolism. *Am. J. Physiol. Ren. Physiol.* **2018**, *314*, F969–F984. [CrossRef] [PubMed]
9. Layton, A.T.; Laghmani, K.; Vallon, V.; Edwards, A. Solute transport and oxygen consumption along the nephrons: Effects of Na⁺ transport inhibitors. *Am. J. Physiol. Ren. Physiol.* **2016**, *311*, F1217–F1229. [CrossRef]
10. Hakimi, S.; Dutta, P.; Layton, A.T. Coupling of renal sodium and calcium transport: A modeling analysis of transporter inhibition and sex differences. *Am. J. Physiol. Ren. Physiol.* **2023**, *325*, F536–F551. [CrossRef]
11. Layton, A. A Complete Set of Equations for a Computational Model of Electrolyte and Water Transport along the Nephrons in a Mammalian Kidney. *bioRxiv* **2022**, bioRxiv:509286. [CrossRef]
12. Layton, A.T.; Vallon, V.; Edwards, A. A computational model for simulating solute transport and oxygen consumption along the nephrons. *Am. J. Physiol. Ren. Physiol.* **2016**, *311*, F1378–F1390. [CrossRef] [PubMed]
13. Alexander, R.T.; Dimke, H. Molecular mechanisms underlying paracellular calcium and magnesium reabsorption in the proximal tubule and thick ascending limb. *Ann. N. Y. Acad. Sci.* **2022**, *1518*, 69–83. [CrossRef] [PubMed]
14. Lee, H.Y.; Topham, D.J.; Park, S.Y.; Hollenbaugh, J.; Treanor, J.; Mosmann, T.R.; Jin, X.; Ward, B.M.; Miao, H.; Holden-Wiltse, J. Simulation and prediction of the adaptive immune response to influenza A virus infection. *J. Virol.* **2009**, *83*, 7151–7165. [CrossRef] [PubMed]
15. Wittner, M.; di Stefano, A.; Wangemann, P.; Nitschke, R.; Greger, R.; Bailly, C.; Amiel, C.; Roinel, N.; de Rouffignac, C. Differential effects of ADH on sodium, chloride, potassium, calcium and magnesium transport in cortical and medullary thick ascending limbs of mouse nephron. *Pflug. Arch.* **1988**, *412*, 516–523. [CrossRef] [PubMed]
16. Quamme, G.A. Control of magnesium transport in the thick ascending limb. *Am. J. Physiol. Ren. Physiol.* **1989**, *256*, F197–F210. [CrossRef]
17. Di Stefano, A.; Wittner, M.; Nitschke, R.; Braitsch, R.; Greger, R.; Bailly, C.; Amiel, C.; Roinel, N.; de Rouffignac, C. Effects of parathyroid hormone and calcitonin on Na⁺, Cl⁻, K⁺, Mg²⁺ and Ca²⁺ transport in cortical and medullary thick ascending limbs of mouse kidney. *Pflug. Arch.* **1990**, *417*, 161–167. [CrossRef] [PubMed]
18. De Baaij, J.H.F.; Hoenderop, J.G.J.; Bindels, R.J.M. Magnesium in Man: Implications for Health and Disease. *Physiol. Rev.* **2015**, *95*, 1–46. [CrossRef] [PubMed]
19. Franken, G.A.C.; Adella, A.; Bindels, R.J.M.; de Baaij, J.H.F. Mechanisms coupling sodium and magnesium reabsorption in the distal convoluted tubule of the kidney. *Acta Physiol.* **2021**, *231*, e13528. [CrossRef]
20. Li, M.; Jiang, J.; Yue, L. Functional Characterization of Homo- and Heteromeric Channel Kinases TRPM6 and TRPM7. *J. Gen. Physiol.* **2006**, *127*, 525–537. [CrossRef]
21. Günther, T.; Vormann, J.; Höllriegel, V. Characterization of Na⁺-dependent Mg²⁺ efflux from Mg²⁺-loaded rat erythrocytes. *Biochim. Biophys. Acta BBA Biomembr.* **1990**, *1023*, 455–461. [CrossRef]
22. Ruat, M.; Snowman, A.M.; Hester, L.D.; Snyder, S.H. Cloned and Expressed Rat Ca²⁺-sensing Receptor: Differential Cooperative Responses to Calcium and Magnesium. *J. Biol. Chem.* **1996**, *271*, 5972–5975. [CrossRef] [PubMed]
23. Bräuner-Osborne, H.; Jensen, A.A.; Sheppard, P.O.; O'Hara, P.; Krosgaard-Larsen, P. The Agonist-Binding Domain of the Calcium-Sensing Receptor Is Located at the Amino-terminal Domain. *J. Biol. Chem.* **1999**, *274*, 18382–18386. [CrossRef] [PubMed]
24. Brown, E.M.; Chen, C.J. Calcium, magnesium and the control of PTH secretion. *Bone Miner.* **1989**, *5*, 249–257. [CrossRef] [PubMed]

25. Riccardi, D.; Valenti, G. Localization and function of the renal calcium-sensing receptor. *Nat. Rev. Nephrol.* **2016**, *12*, 414–425. [[CrossRef](#)] [[PubMed](#)]
26. Murayama, Y.; Morel, F.; Le Grimmellec, C. Phosphate, calcium and magnesium transfers in proximal tubules and loops of henle, as measured by single nephron microperfusion experiments in the rat. *Pflug. Arch.* **1972**, *333*, 1–16. [[CrossRef](#)] [[PubMed](#)]
27. Edwards, A. Regulation of calcium reabsorption along the rat nephron: A modeling study. *Am. J. Physiol. Ren. Physiol.* **2015**, *308*, F553–F566. [[CrossRef](#)]
28. Toka, H.R.; Al-Romaih, K.; Koshy, J.M.; DiBartolo, S.I.; Kos, C.H.; Quinn, S.J.; Curhan, G.C.; Mount, D.B.; Brown, E.M.; Pollak, M.R. Deficiency of the Calcium-Sensing Receptor in the Kidney Causes Parathyroid Hormone-Independent Hypocalciuria. *J. Am. Soc. Nephrol.* **2012**, *23*, 1879. [[CrossRef](#)]
29. Wang, W.H.; Lu, M.; Hebert, S.C. Cytochrome P-450 metabolites mediate extracellular Ca²⁺-induced inhibition of apical K⁺ channels in the TAL. *Am. J. Physiol. Cell Physiol.* **1996**, *271*, C103–C111. [[CrossRef](#)]
30. Wang, W.; Lu, M.; Balazy, M.; Hebert, S.C. Phospholipase A2 is involved in mediating the effect of extracellular Ca²⁺ on apical K⁺ channels in rat TAL. *Am. J. Physiol. Ren. Physiol.* **1997**, *273*, F421–F429. [[CrossRef](#)]
31. Bazúa-Valenti, S.; Rojas-Vega, L.; Castañeda-Bueno, M.; Barrera-Chimal, J.; Bautista, R.; Cervantes-Pérez, L.G.; Vázquez, N.; Plata, C.; Murillo-de-Ozores, A.R.; González-Mariscal, L.; et al. The Calcium-Sensing Receptor Increases Activity of the Renal NCC through the WNK4-SPAK Pathway. *J. Am. Soc. Nephrol.* **2018**, *29*, 1838. [[CrossRef](#)]
32. Hu, R.; McDonough, A.A.; Layton, A.T. Functional implications of the sex differences in transporter abundance along the rat nephron: Modeling and analysis. *Am. J. Physiol. Ren. Physiol.* **2019**, *317*, F1462–F1474. [[CrossRef](#)] [[PubMed](#)]
33. Van Angelen, A.A.; van der Kemp, A.W.; Hoenderop, J.G.; Bindels, R.J. Increased expression of renal TRPM6 compensates for Mg²⁺ wasting during furosemide treatment. *Nephrol. Dial. Transplant. Plus* **2012**, *5*, 535–544. [[CrossRef](#)]
34. Devane, J.; Ryan, M. Diuretics and magnesium excretion. *Magnes. Bull.* **1981**, *3*, 122–123.
35. Ryan, M.P.; Devane, J.; Ryan, M.F.; Counihan, T.B. Effects of diuretics on the renal handling of magnesium. *Drugs* **1984**, *28*, 167–181. [[CrossRef](#)] [[PubMed](#)]
36. Lee, C.-T.; Shang, S.; Lai, L.-W.; Yong, K.-C.; Lien, Y.-H.H. Effect of thiazide on renal gene expression of apical calcium channels and calbindins. *Am. J. Physiol. Ren. Physiol.* **2004**, *287*, F1164–F1170. [[CrossRef](#)] [[PubMed](#)]
37. Costanzo, L.S. Comparison of calcium and sodium transport in early and late rat distal tubules: Effect of amiloride. *Am. J. Physiol. Ren. Physiol.* **1984**, *246*, F937–F945. [[CrossRef](#)]
38. Devane, J.; Ryan, M.P. The effects of amiloride and triamterene on urinary magnesium excretion in conscious saline-loaded rats. *Br. J. Pharmacol.* **1981**, *72*, 285. [[CrossRef](#)]
39. Devane, J.; Ryan, M.P. Dose-dependent reduction in renal magnesium clearance by amiloride during frusemide-induced diuresis in rats. *Br. J. Pharmacol.* **1983**, *80*, 421. [[CrossRef](#)]
40. Friedman, P.A.; Gesek, F.A. Stimulation of calcium transport by amiloride in mouse distal convoluted tubule cells. *Kidney Int.* **1995**, *48*, 1427–1434. [[CrossRef](#)]
41. Chubanov, V.; Ferioli, S.; Wisnowsky, A.; Simmons, D.G.; Leitzinger, C.; Einer, C.; Jonas, W.; Shymkiv, Y.; Bartsch, H.; Braun, A.; et al. Epithelial magnesium transport by TRPM6 is essential for prenatal development and adult survival. *eLife* **2016**, *5*, e20914. [[CrossRef](#)]
42. Mittermeier, L.; Demirkhanyan, L.; Stadlbauer, B.; Breit, A.; Recordati, C.; Hilgendorff, A.; Matsushita, M.; Braun, A.; Simmons, D.G.; Zakharian, E.; et al. TRPM7 is the central gatekeeper of intestinal mineral absorption essential for postnatal survival. *Proc. Natl. Acad. Sci. USA* **2019**, *116*, 4706–4715. [[CrossRef](#)]
43. Verschuren, E.H.; Hoenderop, J.G.; Peters, D.J.; Arjona, F.J.; Bindels, R.J. Tubular flow activates magnesium transport in the distal convoluted tubule. *FASEB J.* **2019**, *33*, 5034–5044. [[CrossRef](#)]
44. Bailly, C.; Roinel, N.; Amiel, C. PTH-like glucagon stimulation of Ca and Mg reabsorption in Henle's loop of the rat. *Am. J. Physiol. Ren. Physiol.* **1984**, *246*, F205–F212. [[CrossRef](#)]
45. Quamme, G.A.; de Rouffignac, C. Renal magnesium handling. In *The Kidney: Physiology and Pathophysiology*; Lippincott Williams & Wilkins: Philadelphia, PA, USA, 2000; p. 375.
46. O'Grady, S.M.; Palfrey, H.C.; Field, M. Characteristics and functions of Na-K-Cl cotransport in epithelial tissues. *Am. J. Physiol. Cell Physiol.* **1987**, *253*, C177–C192. [[CrossRef](#)]
47. Burg, M.B. Tubular chloride transport and the mode of action of some diuretics. *Kidney Int.* **1976**, *9*, 189–197. [[CrossRef](#)] [[PubMed](#)]
48. Di Stefano, A.; Roinel, N.; de Rouffignac, C.; Wittner, M. Transepithelial Ca²⁺ and Mg²⁺ Transport in the Cortical Thick Ascending Limb of Henle's Loop of the Mouse Is a Voltage-Dependent Process. *Ren. Physiol. Biochem.* **2008**, *16*, 157–166. [[CrossRef](#)]
49. Quamme, G.A. Effect of furosemide on calcium and magnesium transport in the rat nephron. *Am. J. Physiol. Ren. Physiol.* **1981**, *241*, F340–F347. [[CrossRef](#)] [[PubMed](#)]
50. Duarte, C.G. Effects of ethacrynic acid and furosemide on urinary calcium, phosphate and magnesium. *Metabolism* **1968**, *17*, 867–876. [[CrossRef](#)]
51. Leary, W.P.; Reyes, A.J.; Wynne, R.D.; van der Byl, K. Renal Excretory Actions of Furosemide, of Hydrochlorothiazide and of the Vasodilator Flosequinan in Healthy Subjects. *J. Int. Med. Res.* **1990**, *18*, 120–141. [[CrossRef](#)] [[PubMed](#)]
52. Brickman, A.S.; Massry, S.G.; Coburn, J.W. Changes in Serum and Urinary Calcium during Treatment with Hydrochlorothiazide: Studies on Mechanisms. *J. Clin. Investig.* **1972**, *51*, 945–954. [[CrossRef](#)] [[PubMed](#)]

53. Kroenke, K.; Wood, D.R.; Hanley, J.F. The Value of Serum Magnesium Determination in Hypertensive Patients Receiving Diuretics. *Arch. Intern. Med.* **1987**, *147*, 1553–1556. [[CrossRef](#)]
54. Stadt, M.M.; Layton, A.T. Adaptive changes in single-nephron GFR, tubular morphology, and transport in a pregnant rat nephron: Modeling and analysis. *Am. J. Physiol. Ren. Physiol.* **2022**, *322*, F121–F137. [[CrossRef](#)]
55. Stadt, M.M.; West, C.A.; Layton, A.T. Effect of pregnancy and hypertension on kidney function in female rats: Modeling and functional implications. *PLoS ONE* **2023**, *18*, e0279785. [[CrossRef](#)]
56. Layton, A.T.; Vallon, V.; Edwards, A. Predicted consequences of diabetes and SGLT inhibition on transport and oxygen consumption along a rat nephron. *Am. J. Physiol. Ren. Physiol.* **2016**, *310*, F1269–F1283. [[CrossRef](#)] [[PubMed](#)]
57. Hu, R.; Layton, A. A computational model of kidney function in a patient with diabetes. *Int. J. Mol. Sci.* **2021**, *22*, 5819. [[CrossRef](#)]
58. Swapnasrita, S.; Carlier, A.; Layton, A.T. Sex-specific computational models of kidney function in patients with diabetes. *Front. Physiol.* **2022**, *13*, 741121. [[CrossRef](#)]
59. Layton, A.T.; Edwards, A.; Vallon, V. Renal potassium handling in rats with subtotal nephrectomy: Modeling and Analysis. *Am. J. Physiol. Ren. Physiol.* **2017**, *314*, F643–F657. [[CrossRef](#)]
60. Stadt, M.M.; Layton, A.T. Mathematical modeling of calcium homeostasis in female rats: An analysis of sex differences and maternal adaptations. *J. Theor. Biol.* **2023**, *572*, 111583. [[CrossRef](#)] [[PubMed](#)]
61. Stadt, M.M.; Leete, J.; Devinyak, S.; Layton, A.T. A mathematical model of potassium homeostasis: Effect of feedforward and feedback controls. *PLoS Comput. Biol.* **2022**, *18*, e1010607. [[CrossRef](#)] [[PubMed](#)]
62. Leete, J.; Layton, A.T. Sex-specific long-term blood pressure regulation: Modeling and analysis. *Comput. Biol. Med.* **2019**, *104*, 139–148. [[CrossRef](#)]
63. Ahmed, S.; Layton, A.T. Sex-specific computational models for blood pressure regulation in the rat. *Am. J. Physiol. Ren. Physiol.* **2020**, *318*, F888–F900. [[CrossRef](#)] [[PubMed](#)]
64. Funato, Y.; Furutani, K.; Kurachi, Y.; Miki, H. CrossTalk proposal: CNNM proteins are Na⁺/Mg²⁺ exchangers playing a central role in transepithelial Mg²⁺ (re)absorption. *J. Physiol.* **2018**, *596*, 743. [[CrossRef](#)] [[PubMed](#)]
65. Arjona, F.J.; de Baaij, J.H. CrossTalk opposing view: CNNM proteins are not Na⁺/Mg²⁺ exchangers but Mg²⁺ transport regulators playing a central role in transepithelial Mg²⁺ (re)absorption. *J. Physiol.* **2018**, *596*, 747. [[CrossRef](#)] [[PubMed](#)]
66. Sponder, G.; Mastrototaro, L.; Kurth, K.; Merolle, L.; Zhang, Z.; Abdulhanan, N.; Smorodchenko, A.; Wolf, K.; Fleig, A.; Penner, R.; et al. Human CNNM2 is not a Mg²⁺ transporter per se. *Pflug. Arch. Eur. J. Physiol.* **2016**, *468*, 1223–1240. [[CrossRef](#)]

Disclaimer/Publisher's Note: The statements, opinions and data contained in all publications are solely those of the individual author(s) and contributor(s) and not of MDPI and/or the editor(s). MDPI and/or the editor(s) disclaim responsibility for any injury to people or property resulting from any ideas, methods, instructions or products referred to in the content.